Broad Next-Generation Integrated Sequencing of Myelofibrosis Identifies Disease-Specific and Age-Related Genomic Alterations

Malathi Kandarpa[1], Dan Robinson[2,3], Yi-Mi Wu[2,3], Tingting Qin[4], Kristen Pettit[1], Qing Li[1,5], Gary Luker[6], Maureen Sartor[4], Arul Chinnaiyan[2,3,7], and Moshe Talpaz[1]

ABSTRACT

Purpose: Myeloproliferative neoplasms (MPN) are characterized by the overproduction of differentiated myeloid cells. Mutations in *JAK2*, *CALR*, and *MPL* are considered drivers of *Bcr-Abl*$^{-ve}$ MPN, including essential thrombocythemia (ET), polycythemia vera (PV), prefibrotic primary myelofibrosis (prePMF), and overt myelofibrosis (MF). However, how these driver mutations lead to phenotypically distinct and/or overlapping diseases is unclear.

Experimental Design: To compare the genetic landscape of MF to ET/PV/PrePMF, we sequenced 1,711 genes for mutations along with whole transcriptome RNA sequencing of 137 patients with MPN.

Results: In addition to driver mutations, 234 and 74 genes were found to be mutated in overt MF ($N = 106$) and ET/PV/PrePMF ($N = 31$), respectively. Overt MF had more mutations compared with ET/PV/prePMF (5 vs. 4 per subject, $P = 0.006$). Genes frequently mutated in MF included high-risk genes (*ASXL1, SRSF2, EZH2, IDH1/2*, and *U2AF1*) and Ras pathway genes. Mutations in *NRAS, KRAS, SRSF2, EZH2, IDH2*, and *NF1* were exclusive to MF. Advancing age, higher DIPSS, and poor overall survival (OS) correlated with increased variants in MF. Ras mutations were associated with higher leukocytes and platelets and poor OS. The comparison of gene expression showed upregulation of proliferation and inflammatory pathways in MF. Notably, *ADGRL4, DNASE1L3, PLEKHGB4, HSPG2, MAMDC2*, and *DPYSL3* were differentially expressed in hematopoietic stem and differentiated cells.

Conclusions: Our results illustrate that evolution of MF from ET/PV/PrePMF likely advances with age, accumulation of mutations, and activation of proliferative pathways. The genes and pathways identified by integrated genomics approach provide insight into disease transformation and progression and potential targets for therapeutic intervention.

Introduction

Essential thrombocythemia (ET), polycythemia vera (PV), and prefibrotic primary myelofibrosis (PrePMF) are phenotypically heterogeneous myeloproliferative neoplasms (MPN), which all carry a risk of progression to overt myelofibrosis (MF; ref. 1). Somatic mutations in JAK2, CALR, or MPL are known drivers of these diseases, but the clinical presentation and outcome of each disease is distinct. Other somatic high-risk mutations including ASXL1, EZH2, IDH1/2, SRSF2, and U2AF1 have also been reported in all MPN, and may bear prognostic significance (2, 3). These secondary hits can be classified in two categories: (i) epigenetic regulators (ASXL1, EZH2, and IDH1/2) and (ii) spliceosome components (SRSF2 and U2AF1). Although ASXL1 mutations alone have prognostic significance in MF, ASXL1 inactivation alone in a mouse model results in myelodysplasia without myelofibrosis (4), and EZH2 deletion in mice results in MF only in a JAK2V617F background and not alone (5). Similarly, how the driver genes and other recurrent somatic mutations interact, leading to MF is yet to be understood. In addition to somatic mutations, there is emerging evidence of germline genetic variants (6) and inflammatory factors (7) that play a role in disease initiation and progression. Evidence of specific pathways that are key regulators of disease progression continues to grow.

The clinical utility of the molecular landscape of MF has been scrutinized, and genetically based prognostic scoring systems have been proposed such as MIPPS70 and GIPPS (8, 9). These models identify high-risk patients and assist in treatment decisions including allogeneic stem cell transplant (alloSCT) and treatment with investigational new drugs, which have a higher risk-to-benefit ratio than conventional therapies. However, the molecular events that drive specific disease phenotypes and explain both clinical features and laboratory findings of each disease are not fully understood. Cytogenetic and molecular profiles of patients with MPN remain difficult to interpret and apply toward personalization of therapy and improving outcomes. This necessitates a more elaborate and extensive genetic characterization of these diseases. Beyond improving outcomes with existing therapies, a clear understanding of the extent and role of mutations beyond the three driver genes can provide new targets for drug discovery for MF.

Unlike ET/PV/PrePMF, MF is an aggressive disease characterized by clonal proliferation of cells in the bone marrow as well as extramedullary sites such as spleen, liver, and lymph nodes. Other signs include excess production of proinflammatory cytokines, progressive bone marrow fibrosis, and a leucoerythroblastic phenotype in the

[1]Division of Hematology/Oncology, Department of Internal Medicine, University of Michigan, Ann Arbor, Michigan. [2]Michigan Center for Translational Pathology, University of Michigan Medical School, Ann Arbor, Michigan. [3]Department of Pathology, University of Michigan Medical School, Ann Arbor, Michigan. [4]Department of Computational Medicine and Bioinformatics, University of Michigan, Ann Arbor, Michigan. [5]Department of Cell and Developmental Biology, University of Michigan, Ann Arbor, Michigan. [6]Department of Radiology, University of Michigan, Ann Arbor, Michigan. [7]Department of Urology, University of Michigan Medical School, Ann Arbor, Michigan.

Corresponding Author: Moshe Talpaz, Department of Internal Medicine, University of Michigan Medical School, 1500 E. Medical Center Dr., Ann Arbor, MI 48109. E-mail: mtalpaz@med.umich.edu

Clin Cancer Res 2024;30:1972–83

doi: 10.1158/1078-0432.CCR-23-0372

Translational Relevance

Mutations in JAK2, CALR, and MPL genes are considered drivers of myeloproliferative neoplasia (MPN), including essential thrombocythemia, polycythemia vera, prefibrotic primary myelofibrosis (MF), and overt MF. Nevertheless, management of prefibrotic MPN compared with overt MF is drastically different, and it is not clear how prefibrotic MPN switches to fibrotic disease with hallmarks of inflammation and bone marrow failure. We hypothesize that there are further genetic events that lead to the transition to overt MF. We therefore studied a broad panel of genes for mutations along with whole-exome RNA-seq in MPN. Our findings (i) provide genetic evidence of MF as a distinct disease as compared with ET/PV/PrePMF based on mutational profile and gene expression, (ii) underscore the need to monitor genetic alterations in MPN beyond the "driver mutations" to predict progression, and (iii) provide rationale to develop therapeutics for MF beyond JAK2 inhibitors, which target proliferative and epigenetic pathways.

peripheral blood. Patients with MF experience debilitating constitutional symptoms (severe fatigue, weight loss, night sweats), massive hepatosplenomegaly, profound cytopenias, risk of transformation to acute leukemia, and significantly shortened life expectancy (10). About 0.8% to 14% of patients with ET/PV/PrePMF will progress to overt MF over 10 to 15 years (11). Most MF patients (85%–90%) harbor acquired mutations in JAK2, MPL, and CALR, like other less aggressive MPN, but this fails to explain the more aggressive nature of MF.

On the basis of clinical presentation, MF clearly represents a progression of ET/PV/PrePMF; nevertheless, molecular mutations and transcriptional and epigenetic events associated with this phenotypic transition are not well defined. To better understand the molecular events that underlie clinical characteristics of MPN and disease pathophysiology, we studied the mutational landscape of >1,700 genes and the gene expression profile of peripheral blood and bone marrow cells, and hematopoietic stem cells from patients with MPN with a focus on MF landscape.

Materials and Methods

Patient sample collection and processing

Patients with malignancies were enrolled in the Mi-ONCOSEQ study, approved by the University of Michigan institutional review board. Eligibility to this study included adults over 18 years and suspected or diagnosed with hematologic malignancies and other cancers. All patients provided written informed consent to genomic research related to this study. The somatic and germline variant report was included in the patient medical records for future use by providers and patients. Peripheral blood samples and/or bone marrow aspirates and buccal swabs were collected from enrolled patients. Bone marrow and peripheral blood mononuclear cells were prepared by Ficoll density gradient centrifugation. To obtain $CD34^+$ cells, mononuclear cells were enriched by incubating with CD34 antibody conjugated to magnetic microbeads and performing MACS separation according to the manufacturer's instructions (Miltenyi Biotec).

Integrative high-throughput clinical sequencing

Nucleic acid preparation, sequencing library construction, and high-throughput sequencing were performed using standard protocols, which adhere to the Clinical Laboratory Improvement Amendments. Paired-end whole-exome libraries from tumor and matched normal DNA were prepared using the Agilent SureSelect human all exon v4 probes (Agilent Technologies). Transcriptome libraries were prepared from total RNA and captured by the Agilent SureSelect human all exon v4 probes (12). All the libraries were sequenced using the Illumina HiSeq2500 (Illumina Inc.). Aligned exome and transcriptome sequences were analyzed to detect putative somatic mutations, insertions, and deletions (indels), copy-number alterations, gene fusions, and gene expression as described previously (13, 14).

Integrative clinical sequencing was performed using standard protocols of the CLIA-compliant (clinical laboratory improvement amendments) sequencing laboratory. Total mononuclear cells or CD34-enriched cells were disrupted by 5-mm beads on a Tissuelyser II (Qiagen). Genomic DNA and total RNA were purified from the same sample using an AllPrep DNA/RNA/miRNA Kit (Qiagen). Matched normal genomic DNA from buccal swabs was isolated using an DNeasy Blood & Tissue Kit (Qiagen). RNA integrity was measured on an Agilent 2100 Bioanalyzer using RNA Nano reagents (Agilent Technologies). RNA sequencing was performed by exome-capture transcriptome platform developed in our lab and as described previously (12). In brief, capture transcriptome libraries were prepared using 1 to 2 μg of total RNA. Following the steps of cDNA synthesis, end-repair, A-base addition, and ligation of adapters, precapture libraries were size-selected by the PippenHT system (Sage Science). Recovered fragments were enriched by PCR using Phusion DNA polymerase (New England Biolabs) and index primers and purified by AMPure XP beads (Beckman Coulter). Coding exons were then captured by Agilent SureSelect Human All Exon v.4 probes following the manufacturer's protocol. Final sequencing libraries were analyzed by Agilent 2100 Bioanalyzer for product size and concentration.

Exome libraries of matched pairs of tumor/normal DNAs were prepared as previously described. In brief, 1 to 3 μg of genomic DNA was sheared using a Covaris S2 to a peak target size of 250 base pairs (bp). Fragmented DNA was concentrated using AMPure beads, followed by end-repair, A-base addition, ligation of the Illumina indexed adapters, and size selection on 3% Nusieve agarose gels (Lonza). Fragments between 300 to 350 bp were recovered, amplified using Illumina index primers, and purified by AMPure beads. One microgram of the library was hybridized to the Agilent SureSelect Human All Exon v.4. The targeted exon fragments were captured and enriched following the manufacturer's protocol (Agilent). Paired-end whole-exome libraries were analyzed by an Agilent 2100 Bioanalyzer and DNA 1000 reagents and sequenced using an Illumina HiSeq 2000 or HiSeq 2500 (Illumina).

FastQC was used to assess read quality per lane. FASTQ conversion was performed with bcl2fastq-1.8.4 in the CASAVA 1.8 pipeline. Picard was used to monitor other sequencing metrics such as duplication rate, GC biases, and targeted coverage.

Somatic and germline mutation calling

The FASTQ files were aligned to the reference genome build hg19, GRCh37 using Novoalign Multithreaded (version 3.02.08; Novocraft) and converted into BAM files using Samtools (ver 0.1.19, RRID: SCR_002105). BAM files were sorted, indexed, and marked for duplicates with Novosort (version 1.03.02). SNV and small indels were called by freebayes (version 1.0.1). Larger indels and exon-level structural arrangements were called with pindel (version 0.2.5b9). The variant calls from freebayes and pindel were compiled, annotated, and matched against the RefSeq database as well as the COSMIC v90, dbSNP v146, ExAC v0.3, and 1000 Genomes phase III databases. This annotation was performed using snpEff and snpSift.

Variant calling was based on tumor-normal variant allele frequency. Following inspection of samples for tumor content using variant allele fractions (VAF) and zygosity shift analysis, samples with less than 10% tumor fraction were excluded from the study.

Determination of regions of uniparental disomy (UPD) begins with the identification of all heterozygous SNP positions in the matched normal sample. Variant fractions are then measured for these SNP in the tumor sample and regions showing loss of heterozygosity are determined. Copy-number status for each region in the tumor sample is determined by coverage ratios of tumor versus matched normal. Regions with LOH and copy-neutral status are classified as acquired UPD.

RNA-sequencing analysis

In total, 129 RNA libraries were generated from PBMC or BMMC samples (EV: 4, PV: 13, Pre-PMF: 7, and MF: 82), or CD34-positive stem cells of MPN (EV: 4, PV: 1, Pre-PMF: 1, and MF: 17), as well as CD34 depleted samples of MF ($n = 5$). The data were assessed for overall quality by FASTQC of each sample followed by TrimGalore processing to trim low-quality bases and adapter sequences. Outlier samples were identified by UMAP clustering (R package umap v 0.2.8.0; https://cran.r-project.org/web/packages/umap/index.html), which showed extreme values at first and second UMAP dimensions (UMAP_1 > 2 and UMAP_2 > 2.5) and excluded from the downstream analysis (Supplementary Fig. S1). The differential gene expression analysis was performed using R package edgeR (version 3.28.1; ref. 15) and the generalized linear model (GLM). Unwanted variance was removed by R package RUVseq (v1.20.0) "ruvr" method (16). The significant differential genes were identified between MF versus others (EV, PV, and pre-PMF) in PBMC/BMMC samples or CD34-enriched samples respectively, or between RAS mutant versus RAS wild-type in PBMC/BMMC samples using the cutoffs of FDR < 0.05 and an absolute fold change ≥2. Gene set enrichment analysis (GSEA) implemented in the Bioconductor package *clusterProfiler* (17) was applied on the log2 fold change ranked gene list using Gene Ontology Biological Process (GOBP) and KEGG pathways (RRID:SCR_012773) with the number of annotated genes greater than 20 and less than 1,000. The significant enriched gene sets were reported using FDR < 0.05.

Statistical analyses

Statistical analysis of the mutation profile and clinical parameters was performed as indicated in GraphPad Prism software (RRID: SCR_002798). All survival analyses were based on log-rank (Mantel–Cox) tests. Overall survival was calculated based on the date of diagnosis as well as based on the date of sample collection (Supplementary Figs. S2A–S2C).

Data availability

Sequencing data from the patients with MPN enrolled in this study can be obtained from the Database of Genotypes and Phenotypes (dbGaP) under accession No. phs000673.v2.p1 (https://www.ncbi.nlm.nih.gov/projects/gap/cgi-bin/study.cgi?study_id=phs000673.v2.p1). The list of genes sequenced in the Mi-Oncoseq panel is presented in Supplementary Table S1. Variant calls in MF and ET/PV/PrePMF are summarized in Supplementary Tables S2 and S3, respectively.

Results

Patient characteristics

A total of 216 patients suspected of ET/PV/PrePMF/MF were recruited to the sequencing study at the University of Michigan over a period of 7 years from 2011 to 2018. Peripheral blood (PB) or bone marrow (BM) samples were collected from patients during a regular clinical care visit in active disease status either on treatment, off treatment, or in between treatments. After thorough review of charts, 163 patients were confirmed for the diagnosis of ET, PV, PrePMF, or MF as per the WHO 2016 diagnosis criteria. Other MPN diagnoses of CML, CNL, and accelerated MF were excluded for this study. Next-generation sequencing (NGS) testing of the 163 patients resulted in 139 samples that were confirmed to have adequate tumor content (see Materials and Methods for details). The patient characteristics of this cohort consisting of 108 MF and 31 ET/PV/PrePMF patients is summarized in **Table 1**. Briefly, the MF cohort had 48 (45%) females and 60 (55%) males with 24 post-ET, 30 post-PV, two post-MPN unclassifiable, and 52 PMF patients. The ET/PV/PrePMF cohort consisted of 14 females (45%) and 17 males (55%). The median age of the MF cohort was 68, whereas for ET/PV/PrePMF, it was 63. As expected from other studies, the clinical presentation of the MF cohort was significantly different from ET/PV/PrePMF with lower hemoglobin levels (10.4 g/dL vs. 12.4 g/dL), a higher leukocyte count (12×10^9/dL vs. 10×10^9/dL), and a higher percentage of high-risk abnormal karyotypes (46% vs. 18%). Furthermore, 54% of MF patients had spleen lengths greater than 7 cm as measured by physical exam, and 90% of the MF patients had a DIPSS score of greater than 1 (18). Driver genes, JAK2, CALR, and MPL were mutated in both cohorts, but notably only the MF cohort had two patients with JAK2 and MPL mutations and four patients with no driver gene mutations, referred to as triple-negative MF.

Table 1. Patient characteristics

	Myelofibrosis	ET/PV/PrePMF
	N = 108	*N* = 31 8 ET, 14 PV, 9 PrePMF
Age at sample: median (range), y	68 (33–85)	63 (43–83)
≤60 y, *N*	29	13
>60 y, *N*	79	18
Sex, female: *N* (%)	48 (45%)	14 (45%)
Hemoglobin: median (range), g/dL	10.4 (5.8–15)	12.4 (10–19.6)
Leukocytes: median (range), 10^9/L	12 (2–203)	10.5 (3–22)
Spleen		
≤7 cm	47	29
>7 cm	56	1
Not determined / splenectomy	3/2	1
Platelets: median (range), K/dL	189 (20–1,006)	436 (134–922)
Precedent disease		
Post-ET	24	N/A
Post-PV	30	
PMF	52	
Post-MPN	2	
DIPSS score		
Low risk	11	N/A
Intermediate 1 risk	30	
Intermediate 2 risk	41	
High risk	26	
Abnormal karyotype	49, 52% (13 ND)	10, 36% (3 ND)
Primary mutations		
JAK2	75	25
CALR	18	5
MPL	13	1
Double	2	0
Triple negative	4	0

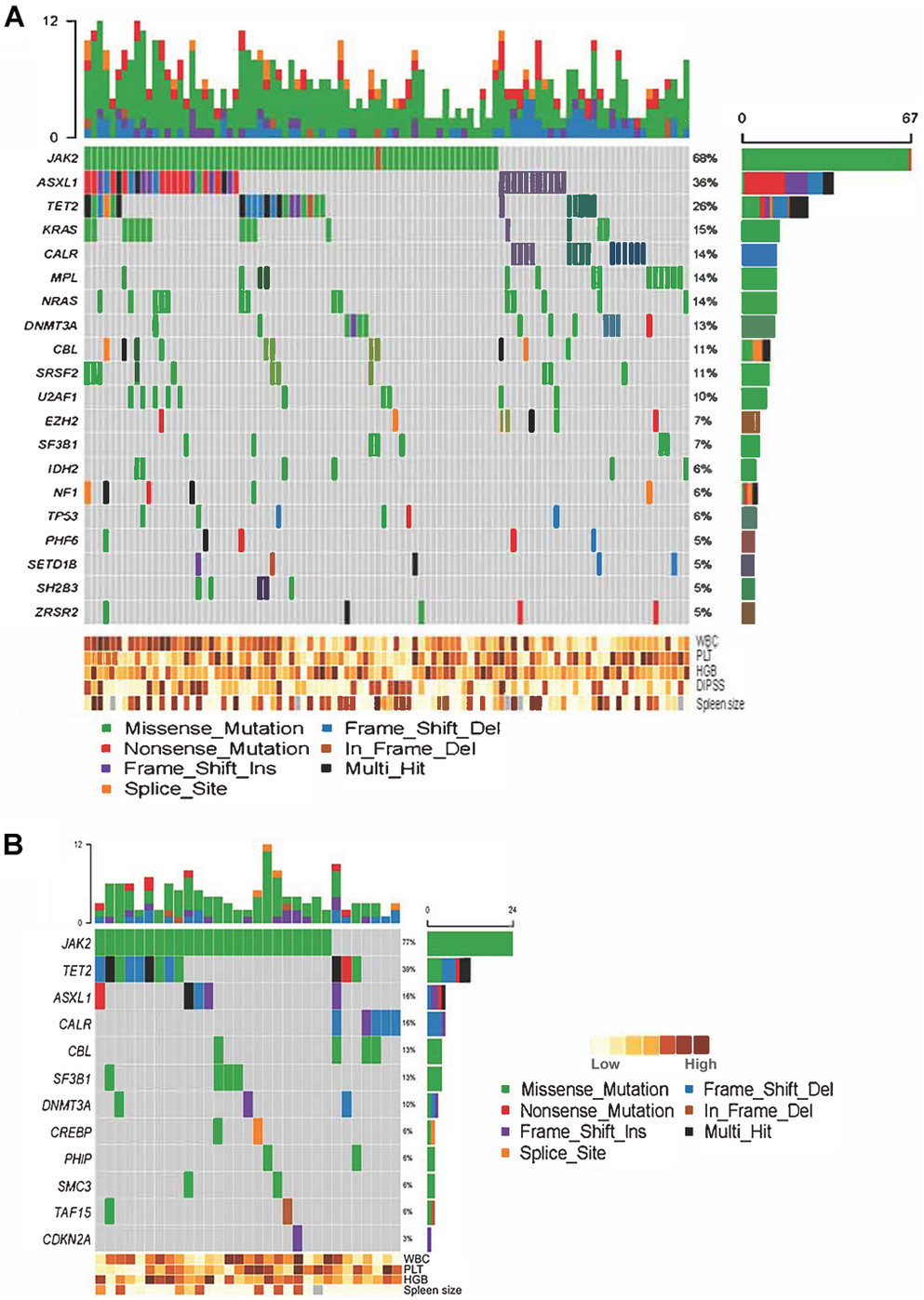

Figure 1.

Oncoplot of the most frequently mutated genes in myelofibrosis and ET/PV/PrePMF. **A,** Summary of the most frequent (>4%) mutations in the MF cohort ($N = 106$) based on a total of 237 genes and 490 unique variants. The Oncoplot arranges patients along the horizontal axis, while genes and their respective mutations are presented vertically for each patient. The plot is divided into four parts: in the upper area is a bar graph of all somatic mutations in each patient: missense, nonsense single-nucleotide variations, frameshift insertions and deletions, in-frame deletions and splice site mutations per patient (see legend for color codes for variant type). The middle panel summarizes all somatic variants found with a frequency of at least 5%. The right-hand panel summarizes the gene variants in a bar graph, and the length of the bar depicts the frequency at which the gene is mutated. The lower panel is a heatmap depiction of clinical parameters of each patient. White blood cell (WBC) count, platelet count (PLT), hemoglobin levels, DIPSS and spleen size are shown. **B,** Summary of the most frequent mutations in the ET/PV/PrePMF cohort ($N = 31$) based on a total of 77 genes and 118 unique variants. The panel descriptions are same as in **A**.

Somatic and germline variations in MPN

A panel of 1,711 genes (Supplementary Table S1) was sequenced to identify somatic and germline variants in the MF and ET/PV/PrePMF cohorts. SNV, indels, and splice site variants were identified. A total of 490 somatic variants were identified in 237 genes for the MF cohort, and a total of 146 somatic variants were identified in 77 genes for the ET/PV/PrePMF cohort. The most frequently altered genes in MF (>6%) and ET/PV/PrePMF (>3%), respectively are summarized in the oncoplots in **Fig. 1A** and **B** (see Supplementary Tables S2 and S3 for a complete list of genes and variants). In the MF cohort, in addition to the frequently mutated genes and variants reported in literature, we also found 215 mutated genes (frequency of <4%) and 271 unique variants. The oncoplots also show disease-related clinical characteristics, WBC count, platelet count, hemoglobin, spleen size, and DIPSS score. Positive trends were observed for JAK2 mutations associating with higher WBC counts and CALR and MPL with higher platelet counts in the MF cohort, but these associations did not reach significance.

MF demonstrated a significantly higher burden ($P = 0.006$) of somatic mutations, with an average of 5.5 mutations per case compared to 4.3 per case in ET/PV/PrePMF (**Fig. 2A**). We also observed an increasing mutation burden from ET (3.1/case) < PV (4.6/case) < prePMF (4.7/case) < overt MF (5.5/case). The distribution in **Fig. 2B** shows the percentage of patients with mutations in each disease.

When we analyzed the mutated genes in both cohorts, we found that only 22 genes, accounting for 7.5% of the total, were shared between them (**Fig. 2C**; Supplementary table S4). We identified 215 unique genes in MF and 55 in ET/PV/PrePMF. The top 25 frequently altered genes in MF are shown in **Fig. 2D**, and for comparison, the incidence of the same in ET/PV/PrePMF is also indicated. The genes that are often mutated exclusively in MF include Ras pathway genes, NRAS, KRAS, CBL, NF1, epigenetic regulators such as DNMT3A, SRSF2, U2AF1, EZH2, SF3B1, IDH2, SH2B3, ZRSR2, SETD1B, and SETBP1, DNA repair pathway TP53, and transcriptional regulators such as ETV6, PHF6, and NOTCH1. Fourteen of the 106 MF patients had germline mutations in the panel of genes sequenced. Of note, eight of the 14

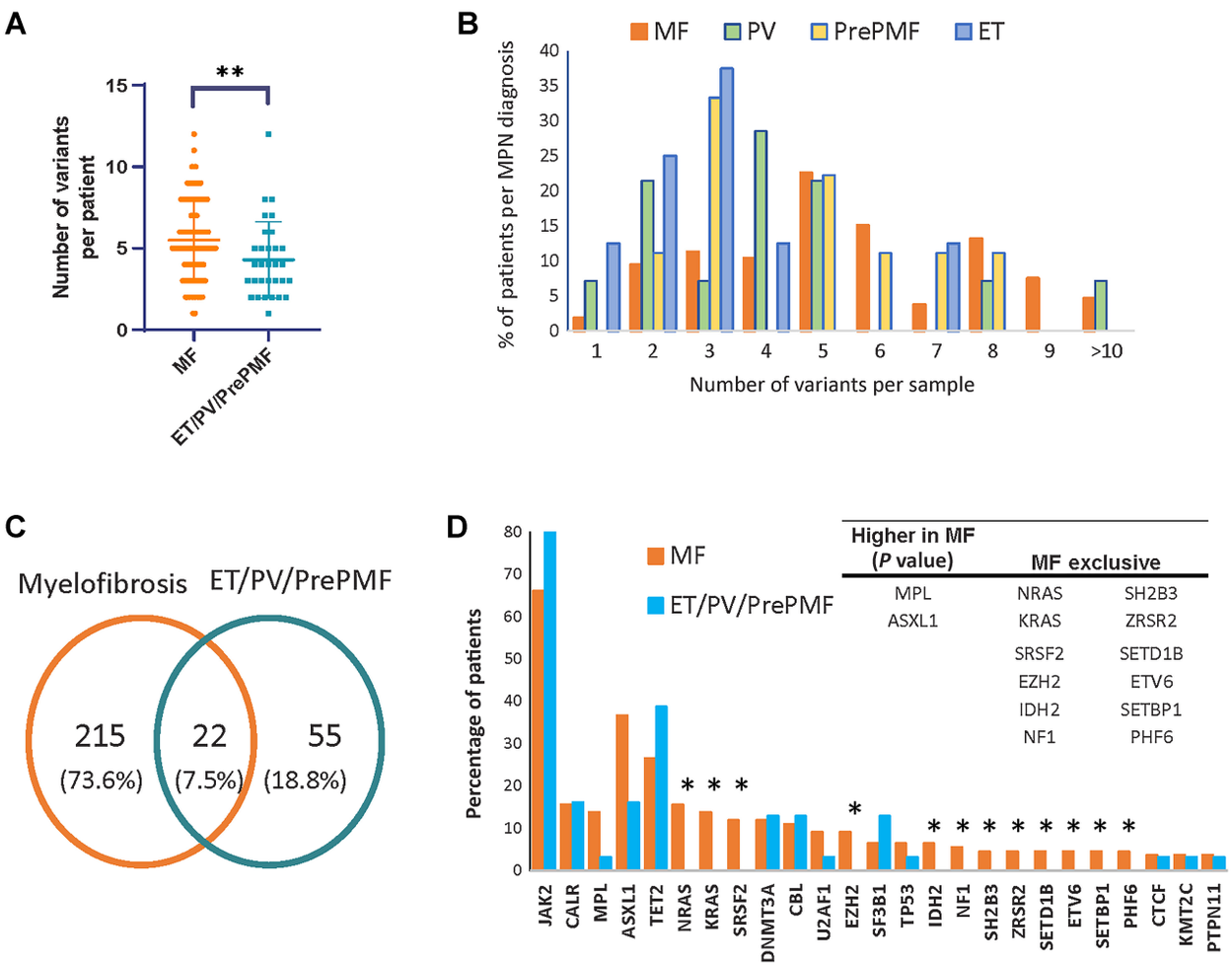

Figure 2.

Somatic gene variants in MPN. **A,** The number of gene variants in MF ($N = 106$) versus ET/PV/PrePMF ($N = 31$). The difference between the two groups was statistically significant ($P = 0.0059$), as calculated by Mann–Whitney test. **B,** Bar chart of the percentage of patients with number of genetic variants in each patient in MF. ET, PV, and PrePMF cohorts. **C,** Venn diagram showing the number of common and distinct sets of genes that are mutated in MF and ET/PV/PrePMF. **D,** The frequency of recurrently mutated genes that occur in more than 4% of MF or ET/PV/PrePMF patients. The asterisk (*) denotes genes that are mutated in MF at a higher rate or exclusively in this cohort. The inset table summarizes these genes.

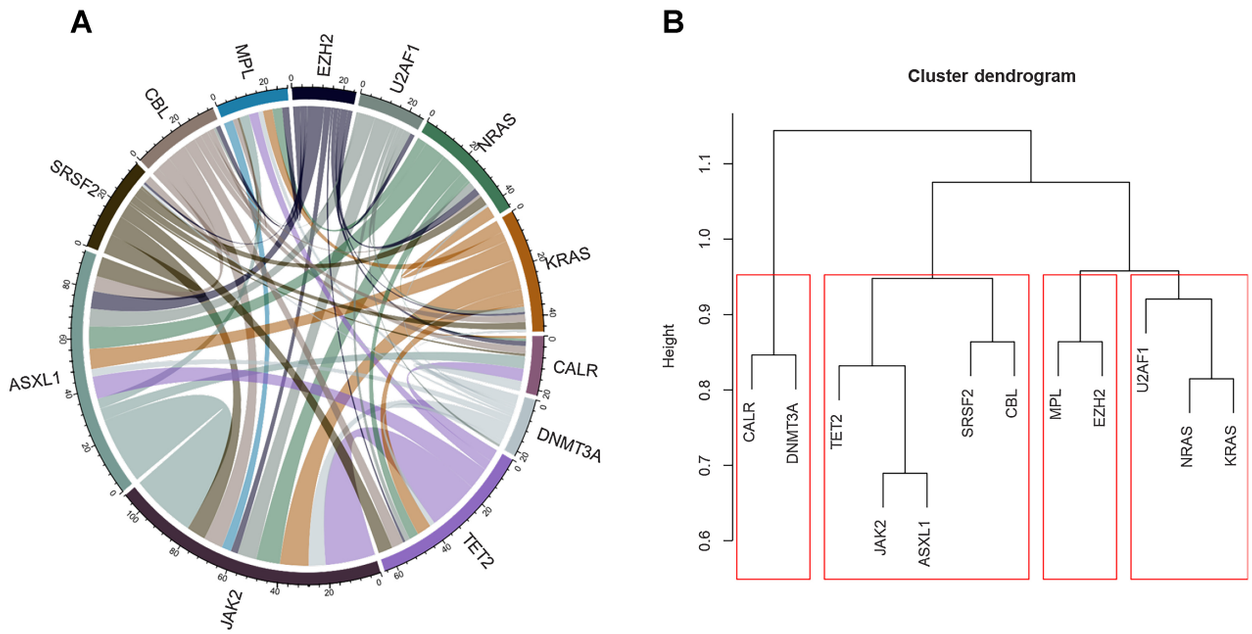

Figure 3.

Mutational complexity in myelofibrosis. A Circos plot (**A**) depicts the relative frequency and pairwise co-occurrence of the top 12 genes mutated in patients with MF. The length of the arc corresponds to the frequency of mutations in the first gene, and the width of the ribbon corresponds to the percentage of patients who also had a mutation in the second gene. Pairwise co-occurrence of mutated genes is denoted only once, beginning with the first gene in the clockwise direction. **B,** The relative co-occurrence of mutated genes in dendrogram form; the genes on the same branch are co-mutated more frequently.

patients had mutations in DNA repair pathway genes ATM/-CHECK/TP53 (Supplementary Table S5). On the other hand, no germline variants were identified in the ET/PV/PrePMF cohort.

Several somatic mutations in the top 12 frequently mutated genes in MF co-occur, as depicted in the Circos plot (A) and the cluster dendrogram (B) in **Fig. 3**. We noted the co-occurrence of variants in low-risk genes such as CALR and DNMT3A (6 of 17 of CALR mutant cases) and the co-occurrence of variants in high-risk genes such as JAK2 and ASXL1 (26 of 72 JAK2 mutant cases). Further, N/KRAS co-occurred preferentially with MPL, EZH2, and U2AF1. Circos and dendrogram analysis was also extended to the top 25 mutated genes (Supplementary Figs. S3A and S3B, respectively).

Age is a significant factor for increased somatic variants in MF patients

The widely used prognostic scoring systems and risk models in MF such as IPSS and DIPSS consider age as a prognostic factor. More recently, mutation-enhanced international prognostic score system (MIPSS) and genetically inspired prognostic scoring system (GIPSS) have been introduced and include clinical and genetic factors in the models but not age. We analyzed the number of somatic mutations as a function of age in our MF cohort and found that they directly correlated (correlation coefficient of 0.8; **Fig. 4A**). This correlation was not evident in the ET/PV/PrePMF cohort. Moreover, the increased number of variants in MF patients was associated with overall survival (OS), with a higher number of variants showing poor survival ($P = 0.0026$; **Fig. 4B**; Supplementary Fig. S2A). The number of variants also correlated with the DIPSS score (**Fig. 4C**), which is agnostic of genotype, suggesting disease severity is a function of age, which in turn, influences genetic instability and increased mutations.

High-risk somatic mutations in ASXL1, EZH2, IDH1/2, SRSF2, and U2AF1 have been reported in MPN, and have been shown to bear prognostic significance (2, 3). Overall survival of older patients with MPN with no mutations in ASXL1 was similar to younger patients with ASXL1 mutations. ASXL1 mutations in older patients showed poor prognosis (**Fig. 4D**; Supplementary Fig. S2C). On the other hand, U2AF1 in younger patients with MPN prognosticates poor survival, and in older patients with MPN, the presence of U2AF1 mutation does not seem to be associated with survival difference (**Fig. 4E**).

UPD and JAK2 allele burden

The early description of acquired UPD came from studies in PV with chromosomal UPD9p and later was linked to JAK2V617F mutation and was reported in other MPN albeit rarely (19). In our MF and ET/PV/PrePMF cohorts, we found a comparable incidence of UPD spanning JAK2V617F (**Fig. 5A**). In addition to JAK2, UPD in CALR, MPL, CBL, EZH2, and SETBP1 were also identified in MF patients. The MF cohort also showed gain of JAK2 due to gene duplication. As would be predicted, due to the complete loss of wild-type JAK2 due to UPD, the VAF for JAK2V617F in MF cases with UPD approached 1.0 (**Fig. 5B**). Previous studies have also reported the relationship of acquired UPD in 9p and allele fraction of JAK2V617F and have proposed two models: (i) expansion of subclone and (ii) emergence of new clones (20). Taken together our data as well as other reports strongly suggest that cells with both mutant JAK2 and acquired UPD have a selective growth advantage that leads to clonal expansion. Although other studies have shown a higher rate of fibrotic transformation related to UPD (21), the presence of UPD may not influence OS in MF or in ET/PV/PrePMF (**Fig. 5C**).

MIPSS and GIPSS consider ASXL1, EZH2, SRSF2, U2AF1, and IDH1/2 genes for risk stratification. The frequency of the Tet2 variant

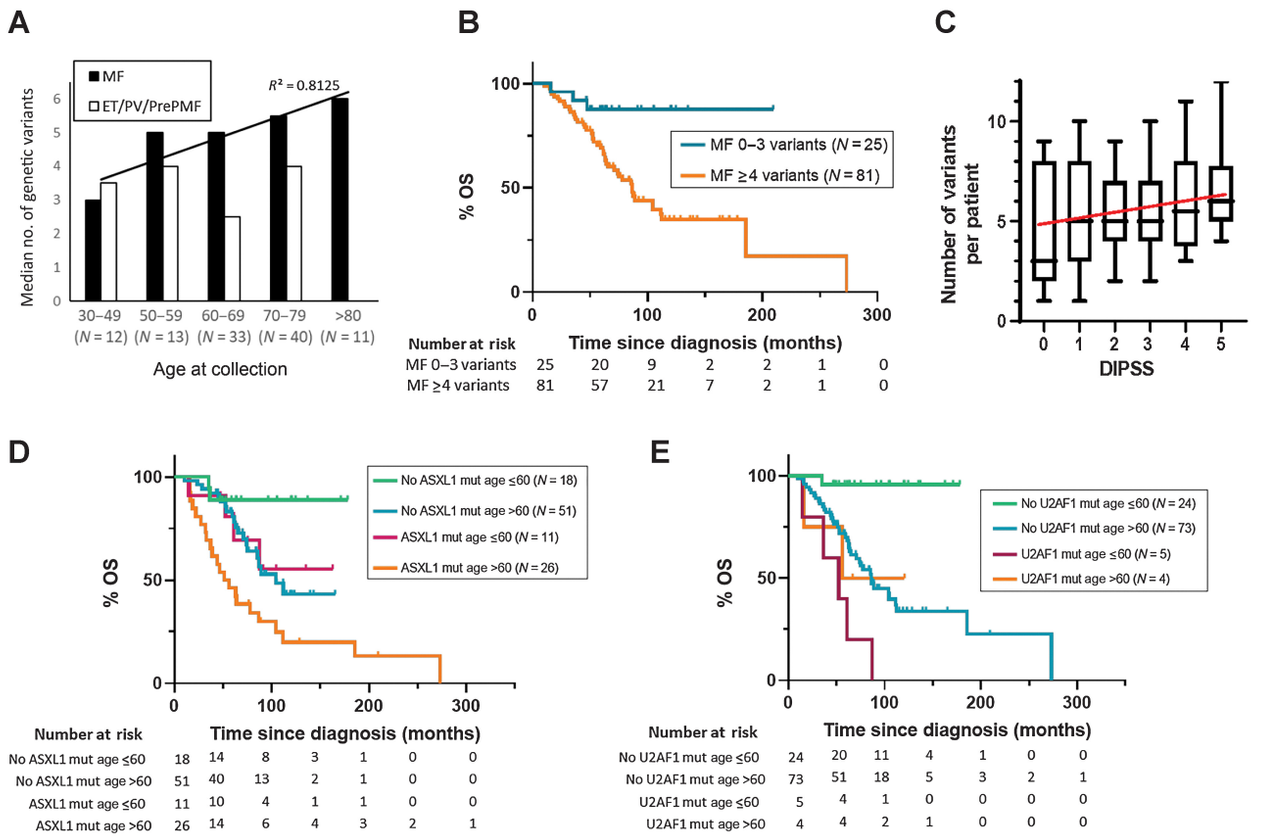

Figure 4.

Correlation of the number of variants with clinical presentation. **A,** The number of genetic variants in different age groups of MF (black bars) and ET/PV/PrePMF patients (open bars). The indicated trendline ($R^2 = 0.8125$) shows a linear relationship of the number of variants with age. **B,** The overall survival rate of MF patients with 0 to 3 variants as compared with >4 variants ($P = 0.0026$). **C,** The number of variants per patient in each DIPSS group. The trendline shows a correlation ($R^2 = 0.88$) of the number of variants with DIPSS. **D,** The percent survival of patients with ASXL1 mutations in ≤60 and >60 age groups as compared with patients without ASXL1 mutation in the same age brackets ($P = 0.0003$). **E** is the same as **D** for U2AF1 gene mutations ($P < 0.0001$).

allele in the MF age group >60 ($N = 23$) was higher than in the age group <60 ($N = 6$; **Fig. 5D**). Higher age correlated with higher VAF ($P = 0.03$) for Tet2, but not for other genes. Nevertheless, KRAS and DNMT3A trended toward higher allele fraction with age but did not reach significance. High-risk genes included in MIPSS and GIPSS along with NRAS, KRAS, CBL, and TP53, all together, also did not show any significant increase in allele fraction with age.

Clinical presentation of MF with Ras family mutations

Ras family mutations have recently been implicated in poor prognosis of MF (22, 23). In our MF cohort, the frequency of Ras family variants, including NRAS, KRAS, CBL, NF1, and MAPK genes, reached 25% of the studied cases (**Fig. 1A**; Supplementary Table S6). These mutations are frequently subclonal alongside a clonal driver mutation background, tumor VAF ranging from 0.01 to 0.95 (**Fig. 6A**). We hypothesized that if Ras is a poor prognostic factor, the clinical presentation of cases with Ras-pathway variants/mutants would be significantly different than with no Ras variants. Although WBC counts ($P = 0.015$) and platelet counts ($P = 0.035$) were significantly higher in Ras mutant MF cases versus nonmutant MF (**Fig. 6B**), hemoglobin levels and spleen size were not significantly different (**Fig. 6B**), and mutations did not have any bearing on DIPSS score (data not shown). Furthermore, Ras pathway mutant patients had poor OS (**Fig. 6C**; Supplementary Fig. S2B). The overall survival of patients, both young (age ≤ 60 years) and old (age > 60 years), with Ras mutations was comparable with older patients with no Ras pathway mutations (**Fig. 6D**).

Gene expression differences in MF versus ET/PV/PrePMF

We studied gene expression using RNA-seq in the 99 MF and 30 ET/PV/PrePMF samples (**Fig. 7A**). To specifically study stem cell compartment changes in MPN, we enriched CD34-positive stem cells from MPN bone marrow aspirates for RNA-seq for a subset of patients. Principal component analysis (PCA) revealed that the gene expression profiles of CD34-positive samples were distinct, but those of the PB and BM cells were indistinguishable (**Fig. 7B**). Therefore, for all further gene expression analysis, we analyzed CD34-positive stem cells separately from PBMC/BMMC. UMAP clustering and RUVr methods were used to remove unwanted variation in the sample; therefore, 14 samples were excluded as outliers (see Materials and Methods section for more details).

Unsupervised hierarchical clustering did not reveal any clear cohorts or MPN subtypes (Supplementary Fig. S4A) or MF subtypes (Supplementary Fig. S4B). We therefore proceeded with differential gene expression analysis (**Fig. 7C–F**, and data summarized in Supplementary Table S7). We first analyzed gene expression patterns in

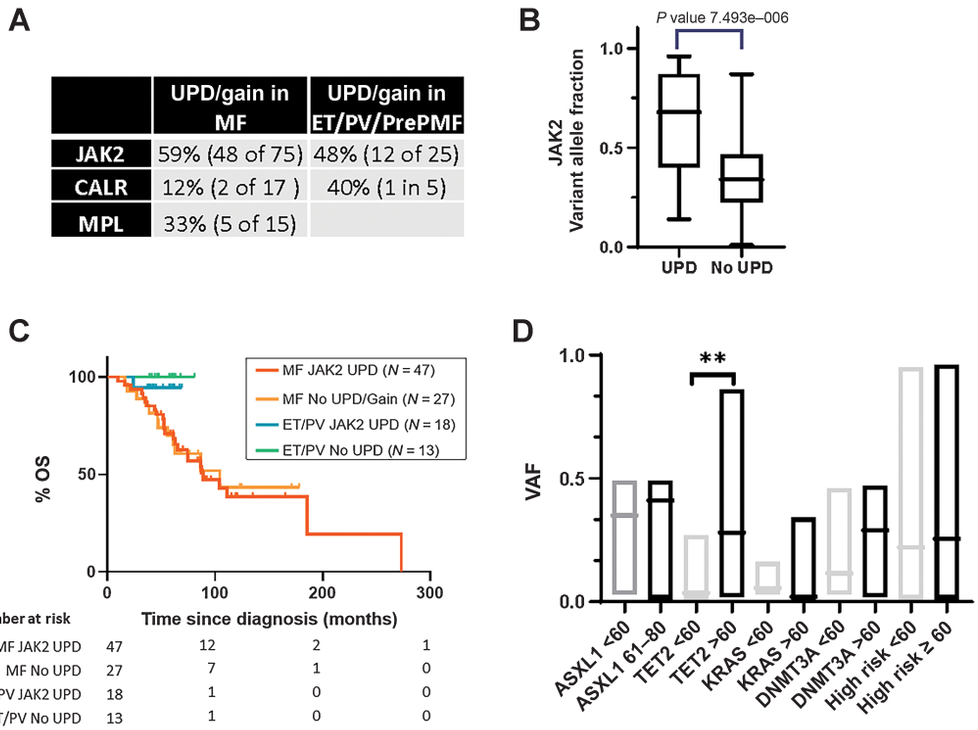

	UPD/gain in MF	UPD/gain in ET/PV/PrePMF
JAK2	59% (48 of 75)	48% (12 of 25)
CALR	12% (2 of 17)	40% (1 in 5)
MPL	33% (5 of 15)	

Figure 5.

UPD and allele burden. **A,** Summarizes the incidence of UPD/gain in the driver genes in MF and ET/PV/PrePMF cohorts. **B,** The relationship between UPD and allele burden. *P* value of 7.4e−006 is based on a *t* test. **C,** The overall survival of patients with UPD/gain in JAK2 compared with patients who did not have UPD/gain in JAK2. **D,** VAF in patients with ASXL1, TET2, KRAS, DNMT3A, and high-risk mutations (see text). Patients are separated based on age to show the relationship of VAF with age. Tet2 VAF was significantly different in patients ≤60 years compared with patients >60 years ($P = 0.005$).

the PBMC/BMMC specimens and found 322 differentially expressed genes between MF versus ET/PV/PrePMF ($P < 0.004$, FDR < 0.05, and FC > 2), including 223 upregulated and 99 downregulated genes (**Fig. 7C** and **E**; Supplementary Table S6). The clinical characteristics such as hemoglobin, white cell count, and spleen size did not distinguish any subset of MPN. The highly downregulated genes (> fourfold) included CLDN4, BMP3, CSMD2, APOD, PDE10A, CCL8, MXRA5, and GPR1. Only genes COL4A5 and PRAME were highly upregulated (>3.5-fold). In comparing gene expression between MF versus ET/PV/PrePMF CD34-positive hematopoietic cells, only nine differentially expressed genes were identified: five highly downregulated (>fourfold; ADGRL4, IL33, TCF7L1, SDC1, and DNASE1L3) and four highly upregulated (>fourfold; HSPG2, PLEKHG4B, MAMDC2, and DPYSL3; **Fig. 7D** and **F**). Although the CD34-positive sample size was small and the number of differentially expressed genes was small, six of the nine genes were also differentially expressed in the PBMC/BMMC sample set (**Fig. 7G**; Supplementary Fig. S5). Genes commonly downregulated in MF CD34 and PBMC/BMMC were ADGRL4 ($P = 4.4E{-}06$) and DNASE1L3 ($P = 1.7E{-}05$). Genes commonly upregulated in MF CD34 and PBMC/BMMC were HSPG2 ($P = 4.9E{-}06$), PLEKHG4B ($P = 2.5E{-}05$), MAMDC2 ($P = 1.8E{-}05$), and DPYSL3 ($P = 1.9E{-}06$).

On the basis of our mutational analysis and clinical correlates, we hypothesize that Ras pathway mutations might be responsible for the aggressive phenotype of MF (**Fig. 6**). We further analyzed if the Ras pathway mutations influence gene expression that underlies proliferative phenotype. Differential gene expression in patients with and without Ras pathway mutations found nine upregulated genes (Supplementary Figs. S6A and S6B) and no downregulated genes. Gene set enrichment analysis in the CD34 enriched stem cells with Ras pathway mutations showed upregulated Ras signaling and PI3K pathway (Supplementary Fig. S6C) both of which have a central role in stem cell activation, cycling, and differentiation (24, 25). The transition to enlarged spleen and extramedullary hematopoiesis is also a hallmark of MF progression; therefore, we studied gene expression in patients with a large spleen (>7 cm below coastal margin by physical exam) versus spleen ≤7 cm (Supplementary Figs. S7A and S7B). Differential gene expression analysis identified 544 upregulated and 303 downregulated genes, and RNA enrichment analysis showed upregulated pathways related to immune response and cell–matrix interactions (Supplementary Fig. S7C).

Discussion

MF is unique among hematologic malignancies, as the hallmark feature of bone marrow fibrosis has both neoplastic contributors (i.e., clonal hematopoiesis and expansion of atypical megakaryocytes) and nonneoplastic contributors (i.e., fibroblast proliferation induced by inflammatory mediators; ref. 26). How and when the disease progresses from a prefibrotic MPN to overt MF is not clear. Driver mutations alone cannot predicate the course of the disease; therefore, we sought to determine what other genetic variants, that is, nondriver mutations and/or gene expression changes, can contribute to the progression from ET/PV/prePMF to MF. We sequenced 1,711 genes, of which 227 were found to be mutated in the MF cohort as compared to 77 in the ET/PV/PrePMF cohort. Nondriver mutations in ASXL1,

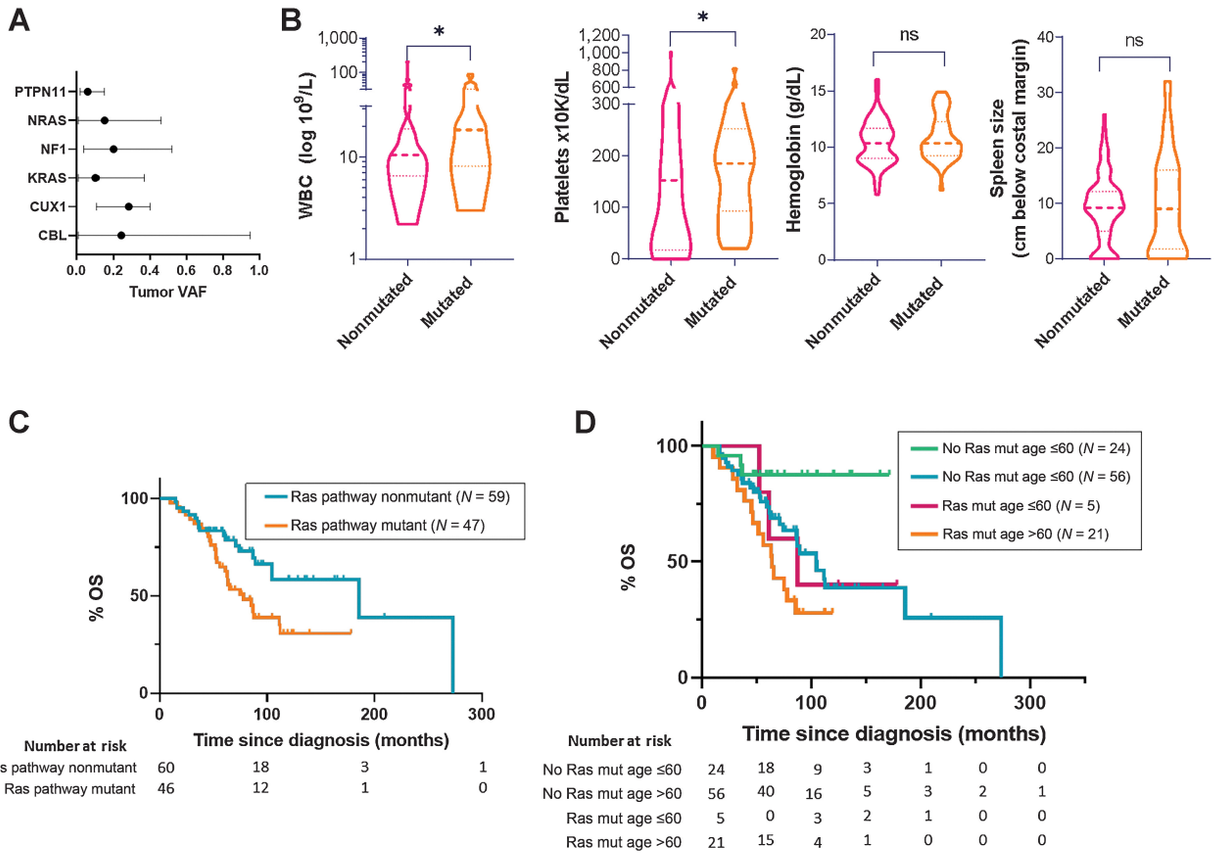

Figure 6.

Impact of Ras pathway gene mutations on clinical presentation in MF. Clinical characteristics of patients with Ras pathway gene (see list of genes in Supplemental materials) mutations were compared with those with wild-type genes. **A,** VAF of Ras pathway mutations in MF patients (CBL $n = 17$, CUX1 $n = 3$, KRAS $n = 17$, NF1 $n = 9$, NRAS $n = 24$, PTPN11 $n = 5$). **B,** WBC, platelets, hemoglobin, and spleen size measured by physical exam, respectively. Differences in WBC count ($P = 0.015$) and platelets ($P = 0.03$) were significant. **C,** The overall survival of patients with Ras pathway mutations compared with patients without these mutations ($P = 0.0154$). **D,** The overall survival of older and younger patients, >60 and ≤60 years, with and without Ras pathway mutations ($P = 0.0078$).

EZH2, TET2, DNMT3A, SRSF2, and U2AF1 genes are frequently detected in MPN and are associated with poor outcomes, in terms of leukemic progression and OS (2) and often referred to as adverse or high-risk variants (3). In this study, EZH2 and SRSF2 variants were only found in the MF cohort and not in the ET/PV/PrePMF cohort (**Fig. 2E**). In addition to the these "high-risk" gene mutations, we also found CBL, NRAS, and KRAS genes were mutated in >10% of cases in the MF cohort, and NRAS and KRAS mutations were limited to the MF cohort.

Age is a common variable in MF prognosis scoring systems such as IPSS (27) and DIPSS (18), which are the two main clinically derived risk models in MF utilized in routine patient management. To better guide treatment options, cytogenetics was incorporated into the DIPSS model, resulting in DIPSS-plus (28), and more recently, both cytogenetics and mutation information were incorporated into MIPSS70-plus (8). The karyotype alterations and gene mutations incorporated in these models are widely seen in many hematologic malignancies (29), as well as in clonal hematopoiesis of indeterminate potential (CHIP), also called age-related clonal hematopoiesis (ARCH). In our sample set, we observed that mutational burden increased with age for some of the high-risk genes. We found that advancing age correlated with increased incidence of mutations in MF patients (**Fig. 4A**). Moreover, high-risk genes were more prevalent in older patients and the allele burden is also higher in older patients (**Fig. 5D**). These data taken together might suggest MF as a progression of CHIP leading to accumulating new mutations in MF patients as evidenced by subclonal mutations and clonal selection as evidenced by increasing allele burden. Therefore, measuring driver mutation allele burden alone is not predictive of transformation to MF, progression of disease, or even treatment response in MF.

The distinguishing top 10% of the genes most frequently mutated in MF notably included NRAS (14%) and KRAS (15%; **Fig. 1A**). Recently, RAS/CBL mutations were noted to predict resistance to JAK inhibitors and were associated with poor prognostic features in MF (22). In addition, MF patients with N/KRAS mutations had shorter 3-year overall survival and a higher incidence of acute myeloid leukemia (23). In our MF data set, we observed correlation of Ras mutations with higher WBC and platelet counts, and no correlations with spleen size, hemoglobin, or DIPSS (**Fig. 6**). RAS variants were reported to be associated with advanced MF features including leukocytosis (23). Higher WBC and platelet counts have also been linked to a proliferative disease that is more likely to progress to AML (30). The question remains if acquisition of Ras mutations along with the canonical driver gene mutations in JAK2, CALR, and MPL, can facilitate the

A

Disease	Cell type	
	CD34 enriched	PBMC/ BMMC
ET	4	4
PV	1	13
PrePMF	1	7
ET/PV/PrePMF	6	24
MF	17	82

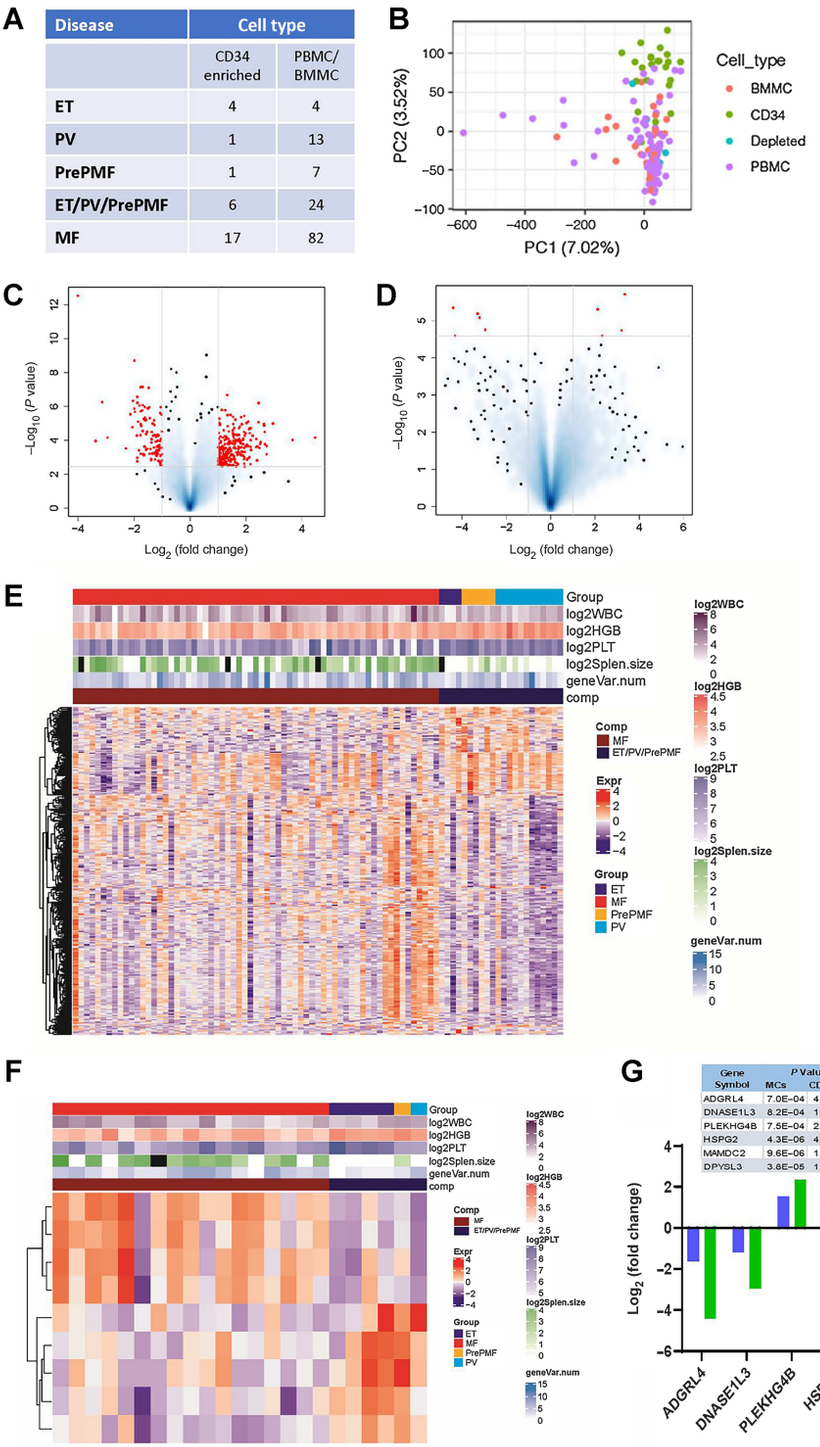

Gene Symbol	*P* Value MCs	CD34
ADGRL4	7.0E−04	4.5E−06
DNASE1L3	8.2E−04	1.7E−05
PLEKHG4B	7.5E−04	2.5E−05
HSPG2	4.3E−06	4.9E−06
MAMDC2	9.6E−06	1.8E−05
DPYSL3	3.8E−05	1.9E−06

Figure 7.

MPN gene expression. Gene expression in ET, PV, PrePMF and MF cells or enriched CD34-positive hematopoietic stem cells was studied by RNA-seq. **A,** Table summarizes the cell types and disease types included in the differential gene expression analyses. **B,** PCA of the gene expression patterns shows clustering of CD34 cells versus the BMMC/PBMC and lymphocyte-depleted PBMC. **C,** A volcano plot illustrates differentially expressed genes between the MF and the ET/PV/PrePMF cohorts when the mononuclear cell (MC) samples were analyzed. The red dots represent 223 genes significantly upregulated and 99 downregulated. **D,** Volcano plot illustrates differentially expressed genes between CD34-positive HSPC from MF versus ET/PV/PrePMF cohorts. The red dots show four genes significantly upregulated and five downregulated. **E,** The heatmap represents gene expression differences of the populations in the volcano plot (**C**), with patients in columns and genes in rows. Clinical characteristics of the patients are shown above the heatmap as a continuous variable or discrete variable as indicated in the figure legend. **F,** A heatmap of gene expression differences of the populations in the volcano plot (**D**); components and labels are the same as in **E**. **G,** Bar graph shows log fold change gene expression of the six genes that were found to be significantly differentially expressed in both the MC and CD34-enriched cells (CD34).

progression of ET/PV/PrePMF to MF. Our data suggest that Ras mutations frequently occur alongside MPL, EZH2, and U2AF1 mutations, as evidenced by the Circos plot and dendrogram for co-occurrence of variants (**Fig. 3**). However, the significance of these co-occurring mutations in disease progression needs to be explored further.

Because driver mutations as well as high-risk mutations such as ASXL1 and TET2 are present both in ET/PV/PrePMF and MF, we studied progression-related gene expression changes in mononuclear cells and CD34-positive hematopoietic stem cells by RNA-seq. Differentially expressed genes in the mononuclear cell compartment were numerous (322 genes) as compared with the CD34 compartment (nine genes), perhaps also due to the smaller sample size. Nevertheless, each of the genes identified as differentially expressed in the CD34 compartments were also differentially expressed in mononuclear cells (**Fig. 7**). Downregulated genes in MF included ADGRL4/ELTD1 and DNASE1L3, which are associated with cardiac fibrosis and internal organ fibrosis, respectively (31, 32). Upregulated genes in MF included PLEKHG4B, HSPG2 MAMDC2, and DPYSL3. HSPG2, also known as perlecan, is implicated in fibrosis as a result of uncontrolled response to inflammation (33), and overexpression of HSPG2 was shown to predict poor survival in AML (34). MAMDC2 was found to be upregulated in CML stem cells and in the ECM during atherogenesis (35, 36). DPYSL3 has been implicated in liver fibrosis and is expressed at higher levels as fibrosis advances (37). In the bone marrow, DPYSL3 is important for osteogenic differentiation of mesenchymal cells and is co-operatively regulated by BMP and Runx2, which are known to play a role in the pathogenesis of myeloid malignancies (38–40).

Gene expression analysis comparing MF with and without RAS pathway mutations identified upregulation of the RAS pathway and PI3K pathway (Supplementary Fig. S6). The RAS–ERK pathway and its crosstalk with the PI3K pathway promote cell survival, growth, proliferation, and plasticity in many different cancers including hematologic malignancies (25, 41). As the evidence for the role of these pathways is accumulating, there are several therapeutic strategies targeting the RAS pathway being explored in clinical trials (42).

Understanding the disease transformation to MF has highlighted many factors: (i) new mutations and accumulating mutations, which may be a result of an unstable genome; (ii) epigenetic regulation, such as chromatin remodeling, which can lead to reprogramming of the hematopoietic system; (iii) aberrant pathway activation such as RAS signaling, which can contribute to proliferative phenotype and further disease transformation; and finally, (iv) inflammation, cytokine secretion, and transformation of medullary and extramedullary stroma to nourish the neoplastic clone. A concerted effort to intervene in these areas holds promise in the treatment and management of MF.

Authors' Disclosures

K. Pettit reports personal fees from AbbVie, Incyte, and Sierra Oncology outside the submitted work. G.D. Luker reports other support from RSNA outside the submitted work and NIH grant funding for studies of imaging methods in myelofibrosis (Nos. R01CA238023 and U24CA237683). M.A. Sartor reports grants from NIH during the conduct of the study and grants from NIH outside the submitted work. M. Talpaz is a scientific advisory board member of BMS, Sierra Oncology, and Sumitomo SDP Oncology. No disclosures were reported by the other authors.

Authors' Contributions

M. Kandarpa: Conceptualization, data curation, formal analysis, supervision, validation, investigation, visualization, methodology, writing–original draft, writing–review and editing. **D. Robinson:** Conceptualization, resources, data curation, software, formal analysis, methodology. **Y. Wu:** Data curation. **T. Qin:** Data curation, software, formal analysis, visualization, methodology, writing–original draft. **K. Pettit:** Formal analysis, validation, writing–review and editing. **Q. Li:** Investigation, writing–review and editing. **G. Luker:** Writing–review and editing. **M. Sartor:** Resources, software, supervision. **A. Chinnaiyan:** Conceptualization, resources, supervision. **M. Talpaz:** Conceptualization, resources, formal analysis, supervision, funding acquisition, project administration, writing–review and editing.

Acknowledgments

We acknowledge the patients who consented to sample collection and sequencing. This research received support from an NIH Clinical Sequencing Exploratory Research Award (NIH 1UM1HG006508). Funding from the D. Dan and Betty Kahn Foundation Grant for Bone Marrow Failure facilitated data analysis, interpretation, and manuscript preparation.

Note

Supplementary data for this article are available at Clinical Cancer Research Online (http://clincancerres.aacrjournals.org/).

Received February 14, 2023; revised May 18, 2023; accepted February 20, 2024; published first February 22, 2024.

References

1. Barbui T, Thiele J, Gisslinger H, Kvasnicka HM, Vannucchi AM, Guglielmelli P, et al. The 2016 WHO classification and diagnostic criteria for myeloproliferative neoplasms: document summary and in-depth discussion. Blood Cancer J 2018;8:15.
2. Vannucchi AM, Lasho TL, Guglielmelli P, Biamonte F, Pardanani A, Pereira A, et al. Mutations and prognosis in primary myelofibrosis. Leukemia 2013;27:1861–9.
3. Tefferi A, Lasho TL, Guglielmelli P, Finke CM, Rotunno G, Elala Y, et al. Targeted deep sequencing in polycythemia vera and essential thrombocythemia. Blood Adv 2016;1:21–30.
4. Abdel-Wahab O, Adli M, LaFave Lindsay M, Gao J, Hricik T, Shih Alan H, et al. ASXL1 mutations promote myeloid transformation through loss of PRC2-mediated gene repression. Cancer Cell 2012;22:180–93.
5. Yang Y, Akada H, Nath D, Hutchison RE, Mohi G. Loss of Ezh2 cooperates with Jak2V617F in the development of myelofibrosis in a mouse model of myeloproliferative neoplasm. Blood 2016;127:3410–23.
6. Bellanné-Chantelot C, Rabadan Moraes G, Schmaltz-Panneau B, Marty C, Vainchenker W, Plo I. Germline genetic factors in the pathogenesis of myeloproliferative neoplasms. Blood Rev 2020;42:100710.
7. Lussana F, Rambaldi A. Inflammation and myeloproliferative neoplasms. J Autoimmun 2017;85:58–63.
8. Guglielmelli P, Lasho TL, Rotunno G, Mudireddy M, Mannarelli C, Nicolosi M, et al. MIPSS70: mutation-enhanced international prognostic score system for transplantation-age patients with primary myelofibrosis. J Clin Oncol 2018;36:310–8.
9. Tefferi A, Guglielmelli P, Nicolosi M, Mannelli F, Mudireddy M, Bartalucci N, et al. GIPSS: genetically inspired prognostic scoring system for primary myelofibrosis. Leukemia 2018;32:1631–42.
10. Mughal TI, Vaddi K, Sarlis NJ, Verstovsek S. Myelofibrosis-associated complications: pathogenesis, clinical manifestations, and effects on outcomes. Int J Gen Med 2014;7:89–101.
11. Barbui T, Thiele J, Passamonti F, Rumi E, Boveri E, Ruggeri M, et al. Survival and disease progression in essential thrombocythemia are significantly influenced by accurate morphologic diagnosis: an international study. J Clin Oncol 2011;29:3179–84.
12. Cieslik M, Chugh R, Wu YM, Wu M, Brennan C, Lonigro R, et al. The use of exome capture RNA-seq for highly degraded RNA with application to clinical cancer sequencing. Genome Res 2015;25:1372–81.

13. Mody RJ, Wu YM, Lonigro RJ, Cao X, Roychowdhury S, Vats P, et al. Integrative clinical sequencing in the management of refractory or relapsed cancer in youth. JAMA 2015;314:913–25.
14. Robinson D, Van Allen EM, Wu YM, Schultz N, Lonigro RJ, Mosquera JM, et al. Integrative clinical genomics of advanced prostate cancer. Cell 2015;161:1215–28.
15. Robinson MD, McCarthy DJ, Smyth GK. edgeR: a bioconductor package for differential expression analysis of digital gene expression data. Bioinformatics 2010;26:139–40.
16. Risso D, Ngai J, Speed TP, Dudoit S. Normalization of RNA-seq data using factor analysis of control genes or samples. Nat Biotechnol 2014;32:896–902.
17. Wu T, Hu E, Xu S, Chen M, Guo P, Dai Z, et al. clusterProfiler 4.0: a universal enrichment tool for interpreting omics data. Innovation (Camb) 2021;2:100141.
18. Passamonti F, Cervantes F, Vannucchi AM, Morra E, Rumi E, Pereira A, et al. A dynamic prognostic model to predict survival in primary myelofibrosis: a study by the IWG-MRT (international working group for myeloproliferative neoplasms research and treatment). Blood 2010;115:1703–8.
19. Kralovics R, Guan Y, Prchal JT. Acquired uniparental disomy of chromosome 9p is a frequent stem cell defect in polycythemia vera. Exp Hematol 2002;30:229–36.
20. Wang L, Swierczek SI, Lanikova L, Kim SJ, Hickman K, Walker K, et al. The relationship of JAK2(V617F) and acquired UPD at chromosome 9p in polycythemia vera. Leukemia 2014;28:938–41.
21. Tefferi A, Lasho TL, Schwager SM, Strand JS, Elliott M, Mesa R, et al. The clinical phenotype of wild-type, heterozygous, and homozygous JAK2V617F in polycythemia vera. 2006;106:631–5.
22. Coltro G, Rotunno G, Mannelli L, Mannarelli C, Fiaccabrino S, Romagnoli S, et al. RAS/CBL mutations predict resistance to JAK inhibitors in myelofibrosis and are associated with poor prognostic features. Blood Adv 2020;4:3677–87.
23. Santos FPS, Getta B, Masarova L, Famulare C, Schulman J, Datoguia TS, et al. Prognostic impact of RAS-pathway mutations in patients with myelofibrosis. Leukemia 2020;34:799–810.
24. Chung E, Hsu C-L, Kondo M. Constitutive MAP kinase activation in hematopoietic stem cells induces a myeloproliferative disorder. PLoS One 2011;6:e28350.
25. Polak R, Buitenhuis M. The PI3K/PKB signaling module as key regulator of hematopoiesis: implications for therapeutic strategies in leukemia. Blood 2012;119:911–23.
26. Nazha A, Khoury JD, Rampal RK, Daver N. Fibrogenesis in primary myelofibrosis: diagnostic, clinical, and therapeutic implications. Oncologist 2015;20:1154–60.
27. Cervantes F, Dupriez B, Pereira A, Passamonti F, Reilly JT, Morra E, et al. New prognostic scoring system for primary myelofibrosis based on a study of the International Working Group for Myelofibrosis Research and Treatment. Blood 2009;113:2895–901.
28. Gangat N, Caramazza D, Vaidya R, George G, Begna K, Schwager S, et al. DIPSS plus: a refined dynamic international prognostic scoring system for primary myelofibrosis that incorporates prognostic information from karyotype, platelet count, and transfusion status. J Clin Oncol 2011;29:392–7.
29. Link DC, Walter MJ. 'CHIP'ping away at clonal hematopoiesis. Leukemia 2016;30:1633–5.
30. Getta BM, Zabor EC, Devlin S, Knapp KM, Patel M, Mohanty A, et al. Pathway mutations are associated with proliferative features and frequently co-occur with TET2 mutations in Philadelphia negative MPN subtypes. Blood 2016;128:4269.
31. Xiao J, Jiang H, Zhang R, Fan G, Zhang Y, Jiang D, et al. Augmented cardiac hypertrophy in response to pressure overload in mice lacking ELTD1. PLoS One 2012;7:e35779.
32. Tsou P-S, Sawalha AH. Unfolding the pathogenesis of scleroderma through genomics and epigenomics. J Autoimmun 2017;83:73–94.
33. Lord MS, Tang F, Rnjak-Kovacina J, Smith JGW, Melrose J, Whitelock JM. The multifaceted roles of perlecan in fibrosis. Matrix Biol 2018;68–69:150–66.
34. Zhou X, Liang S, Zhan Q, Yang L, Chi J, Wang L. HSPG2 overexpression independently predicts poor survival in patients with acute myeloid leukemia. Cell Death Dis 2020;11:492.
35. Avilés-Vázquez S, Chávez-González A, Hidalgo-Miranda A, Moreno-Lorenzana D, Arriaga-Pizano L, Sandoval-Esquivel MÁ, et al. Global gene expression profiles of hematopoietic stem and progenitor cells from patients with chronic myeloid leukemia: the effect of *in vitro* culture with or without imatinib. 2017;6:2942–56.
36. Wierer M, Prestel M, Schiller HB, Yan G, Schaab C, Azghandi S, et al. Compartment-resolved proteomic analysis of mouse aorta during atherosclerotic plaque formation reveals osteoclast-specific protein expression. Mol Cell Proteomics 2018;17:321–34.
37. Hotta K, Kikuchi M, Kitamoto T, Kitamoto A, Ogawa Y, Honda Y, et al. Identification of core gene networks and hub genes associated with progression of non-alcoholic fatty liver disease by RNA sequencing. 2017;47:1445–58.
38. Prashar P, Yadav PS, Samarjeet F, Bandyopadhyay A. Microarray meta-analysis identifies evolutionarily conserved BMP signaling targets in developing long bones. Dev Biol 2014;389:192–207.
39. Toofan P, Wheadon H. Role of the bone morphogenic protein pathway in developmental haemopoiesis and leukaemogenesis. Biochem Soc Trans 2016;44:1455–63.
40. Kuo Y-H, Zaidi SK, Gornostaeva S, Komori T, Stein GS, Castilla LH. Runx2 induces acute myeloid leukemia in cooperation with Cbfβ-SMMHC in mice. Blood 2009;113:3323–32.
41. Braun BS, Tuveson DA, Kong N, Le DT, Kogan SC, Rozmus J, et al. Somatic activation of oncogenic Kras in hematopoietic cells initiates a rapidly fatal myeloproliferative disorder. Proc Natl Acad Sci USA 2004;101:597–602.
42. Song Y, Bi Z, Liu Y, Qin F, Wei Y, Wei X. Targeting RAS–RAF–MEK–ERK signaling pathway in human cancer: current status in clinical trials. Genes Dis 2022;10:76–88.